International Journal of Mechanical, Industrial and Aerospace Sciences
ISSN: 2517-9950
Vol:11, No:3, 2017

Thermal Fracture Analysis of Fibrous Composites with Variable Fiber Spacing Using J_k-Integral

Farid Saeidi, Serkan Dag

***Abstract*—**In this study, fracture analysis of a fibrous composite laminate with variable fiber spacing is carried out using J_k-integral method. The laminate is assumed to be under thermal loading. Jk-integral is formulated by using the constitutive relations of plane orthotropic thermoelasticity. Developed domain independent form of the Jk-integral is then integrated into the general purpose finite element analysis software ANSYS. Numerical results are generated so as to assess the influence of variable fiber spacing on mode I and II stress intensity factors, energy release rate, and T-stress. For verification, some of the results are compared to those obtained using displacement correlation technique (DCT).

***Keywords*—**J_k-integral, variable fiber spacing, thermoelasticity, t-stress, finite element method, fibrous composite.

I. Introduction

ENGINEERING materials are mostly highly sentient to temperature, resulting deformation in the material. Polymer matrix fibrous composites are used widely in industry and their behavior in the case of temperature change is critically important to be analyzed. Composite plates are made of several layers called laminas, and traditionally in fibrous laminas fibers are parallel and uniformly spaced. However, by disturbing isotropy of the laminas by controlling space between fibers to gain more stiffness, where the fibers are laid close to each other, and less density at the regions that fibers have more distance from each other, more efficient laminas than traditional ones can be fabricated [1]. Utilizing composite plates with variable fiber spacing is increasing every day in industry, as a result scientific researches are relatively increasing in this field.

J_k-integral is a pretty useful method, since stress intensity factors (SIFs), T-stress, and also energy release rate can be obtained through, however in calculations based on other methods, obtaining all three factors at the same time is not possible. J_k-integral is a vector defined at the crack tip, and its first component, i.e. J_1, is equivalent to the J-integral [2], [3]. The implementation of J_k-integral is carried out by developing a domain independent form of the formulation at crack tip, in terms of line and area integrals.

The concept of J_k - integral had first been introduced by Knowels et al. [4], Hellen et al. [5], and Budiansky et al. [6], who related path independent J_k-integral to energy release rate associated with cavity or crack rotation, and expansion rate. Four different formulations of J_k-Integral were developed for multifarious engineering materials as a solution for the fracture problems of materials with specific properties. These formulas provide solutions to obtain fracture parameters for thermally loaded homogeneous isotropic solids [7], [8]; homogeneous anisotropic bodies under the effect of mechanical loading [9], [10]; mechanically or thermally loaded bi - material interfaces [11], [12]; functionally graded materials under mechanical or thermal stresses [13], [14].

The objective of this study is to develop an extension of J_k - integral formulation and utilize it as a computational method for calculation of fracture parameters, for fibrous composites with variable fiber spacing subjected to thermal stresses. Constitutive relations of plane orthotropic thermoelasticity were used in developing the J_k - integral formulation for thermal loading; and then shifted to a domain independent form expressed in terms of line and area integrals. Finite element method was used for implementation of new form of J_k-integral. Process of the algorithm designed to obtain thermal fracture parameters solution is carried out using a general purpose finite element program [15]. The computation of fracture parameters in the fibrous composite sheet with variable spaced fiber, involved modeling of an embedded crack in sheet, which is assumed to be in plane stress state and steady state boundary conditions. J_k-integral is used as a numerical method to solve the governing partial equations of thermal field. Some results are presented as a validation for the domain independence of the J_k-integral method, also T-stress and energy release rate is presented as additional crack parameters. Numerical solutions are generated for cracks located in various locations of the composite sheet, also effect of minimum fiber density in the composite sheet, which is changing the function of fiber distribution in the whole sheet is investigate through the same solution for individual models.

II. J_k-Integral Formulation for Thermal Load

A. J_k-Integral and Mechanical Strain Energy Density Function

For both plane stress and plane strain conditions J_k-integral formulation at the crack tip can be written as [16]:

$$J_k = \lim_{\Gamma_\epsilon \to 0} \left(\int_{\Gamma_\epsilon} (W n_k - \sigma_{ij} n_j u_{i,k}) \mathrm{d}s \right) \tag{1}$$

In (1), Γ_ϵ represents an open curve, on which the integration is calculated, illustrated in Fig. 1. The integration curve starts on the lower crack surface and ends on the upper one. In the

Farid Saeidi is with the Department of Aerospace Engineering, Middle East Technical University, and Department of Mechanical Engineering, Atilim University, Ankara 06836, Turkey (phone: +90 312 586 8766; e-mail: farid.saeidi@atilim.edu.tr).

Serkan Dag is with the Department of Mechanical Engineering, Middle East Technical University, Ankara 06800, Turkey (phone: +90 312 210 2580; e-mail: sdag@metu.edu.tr).

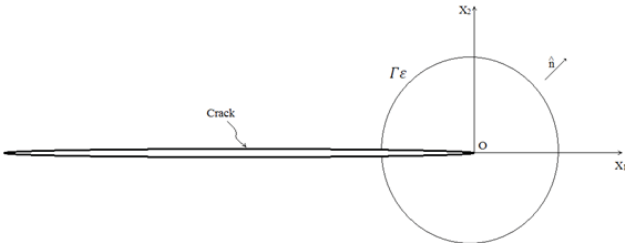

Fig. 1 Intergration path around crack tip

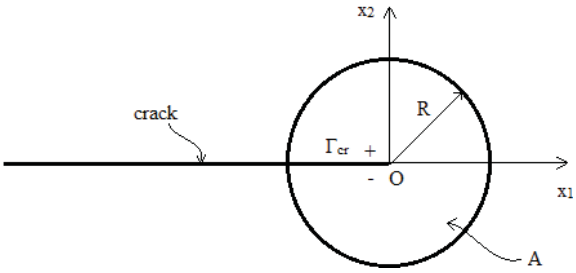

Fig. 2 New integration domains after the change by divergence theorem

equation, n_k, σ_{ij} and s represent outward unit vector, stress tensor and arc length respectively. u_i stands for displacement unit, whereas $u_{i,k}$ represents differentiation, i.e. $()_k \equiv \frac{\partial()}{(\partial x_k)}$. W is the mechanical strain energy density function (3), (4).

$$W = \begin{cases} \frac{1}{2}\sigma_{ij}\epsilon_{ij}^2 \\ \frac{1}{2}\sigma_{ij}\epsilon_{ij}^2 + \frac{1}{2}\sigma_{33}\epsilon_{33}^2 \end{cases} \tag{2}$$

$$W = \frac{E_1^2(\epsilon_{11} - \alpha_1\Delta T) + \nu_{12}E_1E_2(\epsilon_{22} - \alpha_2\Delta T)}{2(E_1 - \nu_{12}^2E_2)}(\epsilon_{11} - \alpha_1 \Delta T) + \frac{\nu_{12}E_1E_2(\epsilon_{11} - \alpha_1\Delta T) + E_1E_2(\epsilon_{22} - \alpha_2\Delta T)}{2(E_1 - \nu_{12}^2E_2)} (\epsilon_{22} - \alpha_2\Delta T) + 2G_{12}\epsilon_{12}^2 \tag{3}$$

$$(\frac{\partial W}{\partial x_k})_{expl} = \frac{\partial W}{\partial E_1}\frac{\partial E_1}{\partial x_k} + \frac{\partial W}{\partial E_2}\frac{\partial E_2}{\partial x_k} + \frac{\partial W}{\partial G_{12}}\frac{\partial G_{12}}{\partial x_k} + \frac{\partial W}{\partial \nu_1}\frac{\partial \nu_1}{\partial x_k} + \frac{\partial W}{\partial \alpha_1}\frac{\partial \alpha_1}{\partial x_k} + \frac{\partial W}{\partial \alpha_2}\frac{\partial \alpha_2}{\partial x_k} + \frac{\partial W}{\partial \beta_1}\frac{\partial \beta_1}{\partial x_k} + \frac{\partial W}{\partial \beta_2}\frac{\partial \beta_2}{\partial x_k} + \frac{\partial W}{\partial \Delta T}\frac{\partial \Delta T}{\partial x_k} \qquad (k = 1, 2) \tag{4}$$

ϵ_{ij}^m is the mechanical strain:

$$\epsilon_{11}^m = \epsilon_{11} - \alpha_1\Delta T \tag{5a}$$
$$\epsilon_{22}^m = \epsilon_{22} - \alpha_2\Delta T \tag{5b}$$
$$\epsilon_{12}^m = \epsilon_{12} \tag{5c}$$

Domain independent form of the integral is found to be in the following form [17]:

$$J_1 = \iint_A (\sigma_{ij}u_{i,1} - W\delta_{1j})q_{,j}\mathrm{d}A - \iint_A (W_{,1})_{expl}q\mathrm{d}A$$

$$J_2 = \iint_A (\sigma_{ij}u_{i,2} - W\delta_{2j})q_{,j}\mathrm{d}A - \iint_A (W_{,2})_{expl}q\mathrm{d}A - \int_{\Gamma_{cr}} (W^+ - W^-)q\mathrm{d}s \quad (i, j = 1, 2) \tag{6}$$

So the integration domain is changed to an area integral A and a line integral Γ_{cr}. Presentation of the integral domain in Fig. 2 shows that Γ_{cr} is actually the crack length surrounded by area A. The shape and the size of the area of the integration should not affect the result of the solution, because this formulation is independent of the domain. In the solution, for validation of this property of the formulation, several circular areas are considered as the integration area.

W^+ and W^- resemble to the strain energy density on the upper and lower face of the crack respectively, Fig. 2.

The solution of the integrals were processed using standard Gauss quadrature, but the only problem with the integral calculation was discontinuity for the $(W^+ - W^-)$ in J_2 expression. The solution for this difficulty was presented by [16], suggesting use of discrete integration on the domain and division of integration interval into two parts, one part is the interval far from crack tip, and the other one would be near crack tip which includes the singularity on the domain. The solution for the second part was reached using asymptotic approximation for mechanical strain energy density difference. The illustration of d as a measurement for determining the close and far parts of the domain is presented in Fig. 3.

$$\int_{\Gamma_{cr}} (W^+ - W^-)q\mathrm{d}\Gamma = \int_0^R (W^+ - W^-)q\mathrm{d}s = \int_0^{R-d} (W^+ - W^-)q\mathrm{d}s + \int_{R-d}^R (W^+ - W^-)q\mathrm{d}s \tag{7}$$

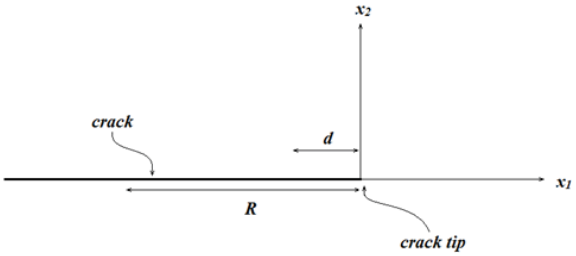

Fig. 3 Representation of d in the model geometry

The solution for the integral near crack tip was achieved using asymptotic distribution of stresses in the region [18].

Expression of difference of W function in polar coordinates would be:

$$W^+ - W^- = W(r, \pi) - W(r, -\pi) \tag{8}$$

From (1), (8) and asymptotic distribution of stress formulation [18]:

$$W(r, \pi) - W(r, -\pi) = (W^+ - W^-) = \frac{1}{2}(a_{11}(\frac{4K_{II}}{\sqrt{2\pi r}}(D(\beta_1^2 - \beta_2^2))T_s)) \tag{9}$$

simplifying (7):

$$(W^+ - W^-) = \frac{1}{\sqrt{2\pi r}} L \tag{10}$$

where:

$$L = 2a_{11} K_{II} [D(\beta_1^2 - \beta_2^2)] T_s \tag{11}$$

Defining following parameters:

$$a_{11} = \frac{1}{E_1} \tag{12}$$

$$D = -\frac{1}{\beta_1 - \beta_2} \tag{13}$$

Then (7) can be written as:

$$\int_{\Gamma_{cr}} (W^+ - W^-) q \mathrm{d}\Gamma \simeq \int_0^{R-d} (W^+ - W^-) q \mathrm{d}s + \int_{R-d}^{R} \frac{L}{\sqrt{2\pi r}} q \mathrm{d}s \tag{14}$$

Simply solving last part of the integral in (14) following equation is obtained:

$$J_2 = \iint_A (\sigma_{ij} u_{i,2} - W\delta_{2j}) q_{,j} \mathrm{d}A - \iint_A (W_{,2})_{expl} q \mathrm{d}A - \int_0^{R-d} (W^+ - W^-) q \mathrm{d}s + 4\sqrt{\frac{d}{2\pi}} \frac{b(3R-d)}{3R} K_{II} T_s \quad (i,j = 1,2) \tag{15}$$

In (15), R is length of the path, integration is calculated over, as shown in Fig. 3, the path near to the crack tip, over which the asymptotic approximation of $(W^+ - W^-)$ is substituted in the main equation, is represented as d, Fig. 3 shows the dimensions in the model. K_{II} is mode II stress intensity factor and T_s stands for T-stress. b is equal to $Im(\mu_1 + \mu_2)$. μ_1 and μ_2 are roots of characteristic equation [18]:

$$a_{11}\mu^4 + (2a_{12} + a_6 6)\mu^2 + a_{22} = 0 \tag{16}$$

In the equation above the constants are equal to the terms below:

$$a_{11} = \frac{1}{E_1}, a_{12} = -\frac{\nu_{12}}{E_1}, a_{22} = \frac{1}{E_2}, a_{66} = \frac{1}{G_{12}} \tag{17}$$

B. Computation of the Crack Parameters Using J_k-Integral Formulation

Considering the final form of J_2 formulation in (15), it can be inferred from equation that the solution cannot be achieved by solving the integral, because K_I, K_{II} and T_s are unknown. In order to find T_s, K_I and K_{II}, a new form of the equation is presented for $\tilde{J}_2$ [16]:

$$\tilde{J}_2^1 = J_2 - \sqrt{d_1}[1 - \frac{d_1}{3R}]S \tag{18}$$

$$\tilde{J}_2^2 = J_2 - \sqrt{d_2}[1 - \frac{d_2}{3R}]S \tag{19}$$

Equations above are $\tilde{J}_2$ written for two different values of d, which allow us to evaluate the values of S and J_2 through a linear equation system. The values given to d where defined dependent on the crack length and these values are equal to $d_1 = 0.0001a$ and $d_2 = 0.0002a$. In these simplified equations the approximation is presented in terms of one variable:

$$S = \frac{4Im(\mu_1 + \mu_2) a_{11}}{\sqrt{2\pi} K_{II}} T_s \tag{20}$$

Then solution for S and J_2 would be:

$$J_2 = \frac{\sqrt{d_1}(1 - \frac{d_1}{3R})\tilde{J}_2^1 - \sqrt{d_2}(1 - \frac{d_2}{3R})\tilde{J}_2^2}{\sqrt{d_1}(1 - \frac{d_1}{3R}) - \sqrt{d_2}(1 - \frac{d_2}{3R})} \tag{21}$$

$$S = \frac{\tilde{J}_2^1 - \tilde{J}_2^2}{\sqrt{d_1}(1 - \frac{d_1}{3R}) - \sqrt{d_2}(1 - \frac{d_2}{3R})} \tag{22}$$

After getting S and J_2, T-stress can be calculated from (10), (11), (13) and (20).

$$T_s = \frac{s\sqrt{2\pi}}{4a_{11} K_{II} D(\beta_1^2 - \beta_2^2)} \tag{23}$$

Since J_1 and $\tilde{J}_2$ are solved only using numerical method for the integral, and solving the equation system, we obtain J_2 and S. As an additional equation, to make system of the unknowns solvable, we use the relation between J_1 and J_2 [18]:

$$J_1 = B_1 K_I^2 + B_2 K_{II}^2 \tag{24}$$

$$J_2 = B_3 K_I K_{II} \tag{25}$$

where:

$$B_1 = -\frac{a_{11}}{2} Im((\mu_1 + \mu_2)\overline{\mu_1 \mu_2}) = \frac{a_{11}}{2}(\beta_1 + \beta_2)(\beta_1 \beta_2) \tag{26a}$$

$$B_2 = \frac{a_{11}}{2} Im(\mu_1 + \mu_2) = \frac{a_{11}}{2}(\beta_1 + \beta_2) \tag{26b}$$

$$B_3 = -a_{11}(\beta_1 + \beta_2)(\beta_1 \beta_2) \tag{26c}$$

Equations (24) and (25) clearly show that K_I and K_{II} are coupled, so this system of equations for intensity factors can be solved using numerical methods. Kim and Paulino [18] have used Newton iteration method to find intensity factors, but in this method they needed to have initial values for SIFs. These initial values were obtained using DCT (Displacement Correlation Technique). However, in this study the values for μ_k were all purely imaginary, because directions of axes coincide with principle directions of elasticity and crack is laying on one of the principle orthotropy directions. In equations above, $\overline{\mu_1}$ and $\overline{\mu_2}$ are representing the conjugates of μ_1 and μ_2 in the equation.

Defining K_I in terms of K_{II}, one can write:

$$K_I = -\frac{J_2}{K_{II} a_{11}(\beta_1+\beta_2)\beta_1\beta_2} \tag{27}$$

$$K_{II}^4 - \frac{2J_1}{a_{11}(\beta_1+\beta_2)} K_{II}^2 + (-\frac{J_2}{a_{11}(\beta_1+\beta_2)\beta_1\beta_2})^2\beta_1\beta_2 = 0 \tag{28}$$

System of equations above was solved as below:

$$K_I = \pm\sqrt{\frac{J_1}{2B_1}[1 \pm \sqrt{1 - \frac{4B_1B_2}{B_3^2}(\frac{J_2}{J_1})^2}]} \tag{29}$$

$$K_{II} = \frac{J_2}{B_3 K_I} \tag{30}$$

Once K_{II} is calculated from the equation above T-stress can be determined using (23). In order to determine the right sign for the intensity factors, a method based on relative normal and tangential displacements of two nodes, defined very close to the crack tip was manipulated [19]. Investigating displacements of nodes close to crack tip will truly show if either $-$ or $+$ sign should be assigned for intensity factors. Two couples of nodes at both upper and lower crack faces were chosen, then [18]:

$$\Delta_1 = u_2^+ - u_2^2 \tag{31}$$

$$\Delta_2 = u_1^+ - u_1^2 \tag{32}$$

A positive outcome for Δ_1 implies that K_I should be positive, which shows crack is open, and if Δ_2 is positive K_{II} should be positive too. In ((31)) and ((32)), the signs in the parenthesis should also be determined [20]:

If $|\Delta_1| \geq |\Delta_2|$ take $+$ for K_{II} and $-$ for K_I
If $|\Delta_1| \leq |\Delta_2|$ take $-$ for K_{II} and $+$ for K_I

III. Problem Description and Numerical Results

For thermal fracture analysis of the orthotropic composite, a crack was embedded in the fibrous composite as illustrated in Fig. 4. x_1 and x_2 are two principal axes of the sheet, and fiber volume was assumed to change along x_2 axis of the medium. V_{f_0} and V_{f_w} are minimum and maximum fiber volumes in the composite sheet respectively. The extrema of the volume were considered to be at the lower and upper boundaries of the medium. Boundary conditions for the problem are illustrated in Fig. 5, T resembles thermal boundary condition. The problem is solved for cracks embedded in different locations of the composite sheet, 0.1, 0.2, 0.3 and 0.4 were taken as the value of h_1; consequently four different models were simulated and analyzed. Volume of the fiber is assumed to be a function of x_2 and also P, as it can be seen obviously from ((33)), V_{f_0} took values equal to 0.1, 0.2, 0.3 and 0.4, and V_{f_w} had the value of 0.7 through calculations. In ((33)), P as an exponent defines the properties of the sheet, so by changing P from 0 to infinity during calculations, solution will be done for several models. Considering both physical and material models, solutions were done for 256 different mediums.

$$V_f(x_2) = V_{f_0} + (V_{f_w} - V_{f_0})(\frac{x_2}{h})^P \tag{33}$$

$$V_m(x_2) = 1 - V_f(x_2) \tag{34}$$

In the equations above V_f stands for volume of the fiber and V_m stands for volume of the matrix.

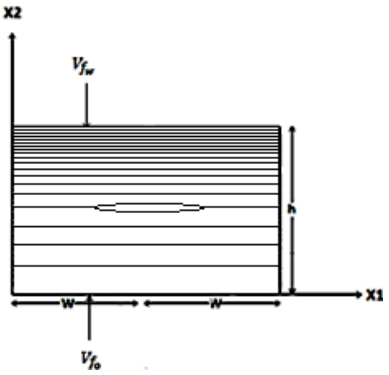

Fig. 4 Crack embedded in fibrous composite with variable fiber spacing

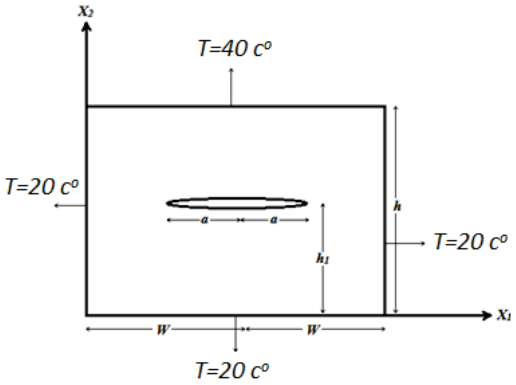

Fig. 5 Boundary conditions for the problem

The solution of the problem is achieved by finding the solution for the half of the actual medium, since the medium is symmetric in x_1 direction. Thus simulating a half model with an insulated boundary condition in the cut face would give us the desired solution. So the whole process during simulation and solution is carried out for crack at $x_1 = a$, but after finding crack parameters at this crack tip we can find the parameters for the other one as shown below:

$$J_1(-a) = J_1(a) \tag{35a}$$
$$J_2(-a) = J_2(a) \tag{35b}$$
$$T_s(-a) = T_s(a) \tag{35c}$$

Orthotropic materials are materials having two or three planes of symmetry; such a characteristic fits properties of the material used in this study, so the composite sheet used is

a non-homogenous orthotropic material. For such a material the thermal constitutive relations under plane stress condition can be written as:

$$\begin{pmatrix} \epsilon_1 \\ \epsilon_2 \\ \epsilon_3 \end{pmatrix} = \begin{bmatrix} 1/E_1 & -\nu_{12}/E_1 & 0 \\ \nu_{12}/E_1 & 1/E_1 & 0 \\ 0 & 0 & 1/G_{12} \end{bmatrix} \begin{pmatrix} \sigma_1 \\ \sigma_2 \\ \sigma_{12} \end{pmatrix} + \begin{pmatrix} \alpha_1 \\ \alpha_2 \\ 0 \end{pmatrix} \Delta T \quad (36)$$

In the equation above ϵ_{ij} are the strain tensor elements. σ_{ij} are stresses and ΔT is thermal variation at the point. This variation is calculated with respect to T_0, which is initial reference value causing no strain in the medium. α is the thermal expansion coefficient. Mechanical properties of the fibrous composites are defined as:

$$E_1(x_2) = E_f V_f(x_2) + E_m V_m(x_2) \quad (37a)$$

$$\frac{1}{E_2(x_2)} = \frac{V_f(x_2)}{E_f(x_2)} + \frac{V_m(x_2)}{E_m} \quad (37b)$$

$$\frac{1}{G_{12}(x_2)} = \frac{V_f(x_2)}{G_f} + \frac{V_m(x_2)}{G_m} \quad (37c)$$

$$\alpha_1(x_2) = \frac{1}{E_1(x_2)}(\alpha_f E_f V_f(x_2) + \alpha_m E_m V_m(x_2)) \quad (37d)$$

$$\alpha_2(x_2) = (1+\nu_f)\alpha_f V_f(x_2) + (1+\nu_m)\alpha_m V_m(x_2) - \alpha_1(x_2)\nu_{12} \quad (37e)$$

$$k_1(x_2) = k_f V_f(x_2) + k_m V_m(x_2) \quad (37f)$$

$$k_2(x_2) = \frac{1+\eta V_f(x_2)}{1-\eta V_f(x_2)} k_m \quad (37g)$$

$$\eta = \frac{\frac{k_f}{f_m} - 1}{\frac{k_f}{k_m} + 1} \quad (37h)$$

$$D_1(x_2) = D_m V_m(x_2) \quad (37i)$$

$$D_2(x_2) = (1 - 2\sqrt{\frac{V_f(x_2)}{\pi}}) D_m \quad (37j)$$

In the equations above, m and f stand for matrix and fiber property in the sheet respectively.

In the following section tables show both comparison of the results with DCT technique and also the superposition of the results are presented.

As previously presented in Figs. 4 and 5, a fibrous composite sheet with variable spaced fiber and a crack with length of $2a$ is embedded in different locations of the plate in various analysis. $T_r = T_0$ is defined as reference temperature and as shown in Fig. 5, temperature at boundary of $X_2 = h$ is equal to $2T_0$, and on the other boundaries, it is equal to T_0. The crack faces are assumed to be insulated, and that means no thermal flux is provided at these faces. Considering all the analysis in this paper, most of the variables are changing in different models, but for all the models T_0, h and W remain the same and equal to $T_0 = 20$, $h = 2.5$ and $W = 5$. In (37j), m and f in the variables show the relation of the property with matrix and fiber material respectively. α shows the thermal expansion. Matrix is chosen to be epoxy and fibers in the matrix are glass fiber. Properties for these materials are presented in Table I.

TABLE I
MATERIAL PROPERTIES FOR MATRIX AND FIBER

Paroperty	Epoxy matrix	Glass Fiber
$E(GPa)$	3.4	85
$G(GPa)$	1.308	35.42
ν	0.3	0.2
$\alpha(1/^0C)$	$63(10)^{-6}$	$5(10)^{-6}$
$\rho(Kg/m^3)$	1200	2500
$k(W/m^0C)$	0.25	1.05
$D(m^2/s)$	$3(10)^{-15}$	N/A

Calculations are carried out using different domain circles, the domain independency of J_k-integral is proven using outcomes of solutions for different domains; however, a validation for the results gained using J_k-integral is needed. For this purpose, Table II is prepared to show both the results achieved using J_k-integral and results for the same model achieved using another method called displacement correlation technique (DCT) [18], [21]. For presentation of the results some kind of normalization of the data was required, thus in all the results (38d) was used to make result normalized.

$$K_{In} = \frac{K_I}{a_m E_m T_0 \sqrt{\pi a}} \quad (38a)$$

$$K_{IIn} = \frac{K_{II}}{a_m E_m T_0 \sqrt{\pi a}} \quad (38b)$$

$$J_{In} = \frac{J_I}{a_m^2 E_m T_0^2 \pi a} \quad (38c)$$

$$T_{sn} = \frac{T_s}{a_m E_m T_0} \quad (38d)$$

Deformed medium under effect of thermal loads can be observed in the following figures. In Fig. 6 mesh map and distribution around at the crack tip and through the medium is presented.

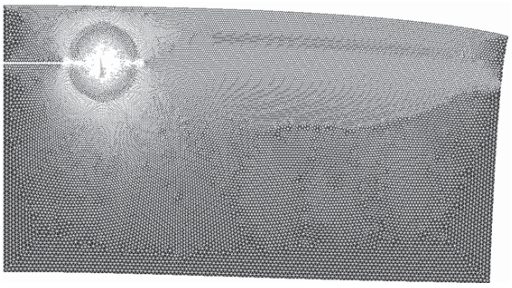

Fig. 6 Deformation and mesh map of the simulated model

It is clear from the tables that DCT and J_k-integral give out nearly the same results, which admits the validity of them. Last column in Table II, shows the difference between results of two methods.

Some of the graphs for the interpretation of the results for solution of the mediums with various dimensions and crack location, and also several values for the minimum and

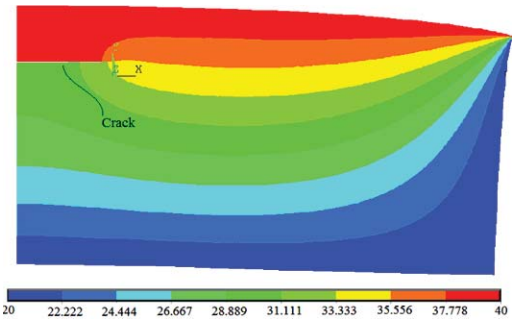

Fig. 7 Contour plot illustrating temperature distribution on the medium and structural deformation caused by thermal load

TABLE II
RESULTS OF PLAIN STRESS THERMAL SOLUTION FOR THE MODEL
$w = 5, h = 2.5, h_1 = 2, a = 1, V_{f_0} = 0.1, P = 0.1$

	DCT		J_k-integral	
R/a	K_I	K_{II}	K_I	K_{II}
0.1	0.02202	0.05662	0.02198	0.05707
0.2	0.02202	0.05662	0.02201	0.05705
0.3	0.02202	0.05662	0.02101	0.05704
0.4	0.02202	0.05662	0.02202	0.05704
Thermal				

maximum fiber volume at the lower and upper boundaries are presented below.

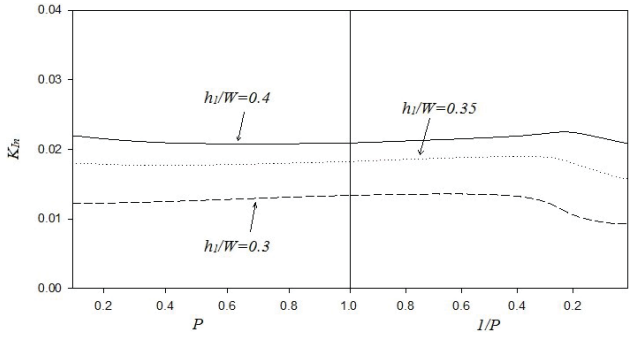

Fig. 8 Normalized first mode SIF for the model
$w = 5, h = 2.5, a = 1, V_{f_0} = 0.1$

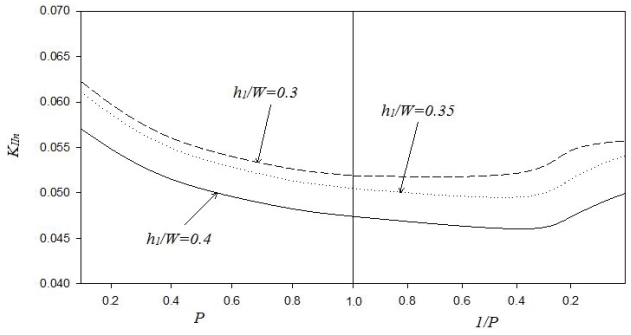

Fig. 9 Normalized second mode SIF for the model
$w = 5, h = 2.5, a = 1, V_{f_0} = 0.1$

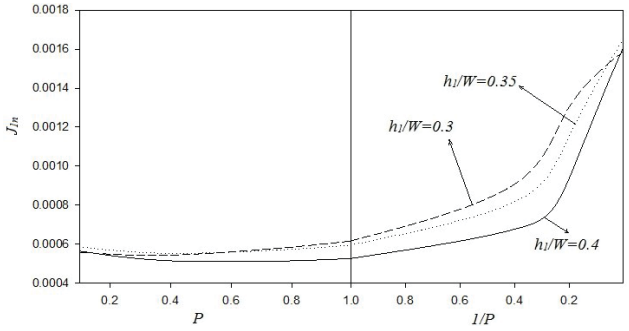

Fig. 10 Normalized energy release rate for the model
$w = 5, h = 2.5, a = 1, V_{f_0} = 0.1$

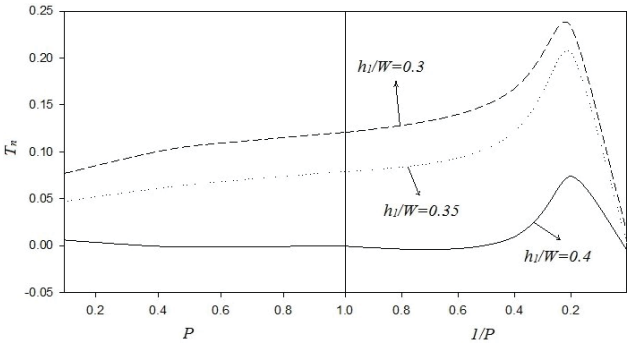

Fig. 11 Normalized T-stress for the model
$w = 5, h = 2.5, a = 1, V_{f_0} = 0.1$

Following graphs show affect of crack length on the fracture parameters:

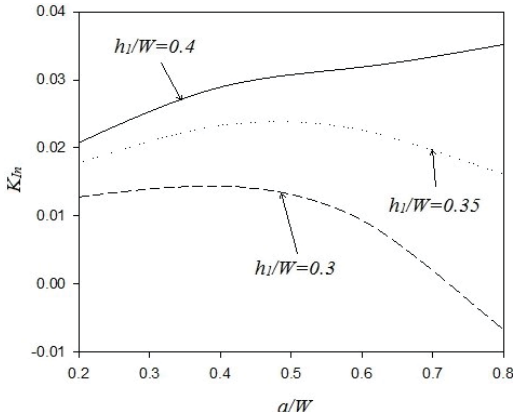

Fig. 12 Normalized first mode SIF for the model
$w = 5, h = 2.5, P = 0.6, V_{f_0} = 0.1$

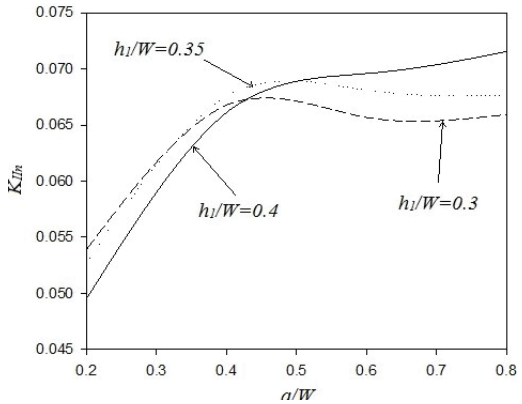

Fig. 13 Normalized second mode SIF for the model $w = 5, h = 2.5, P = 0.6, V_{f_0} = 0.1$

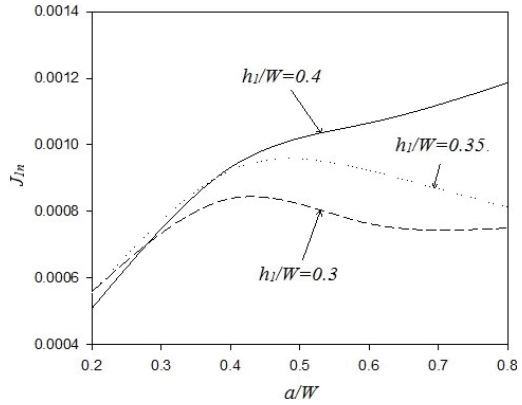

Fig. 14 Normalized energy release rate for the model $w = 5, h = 2.5, P = 0.6, V_{f_0} = 0.1$

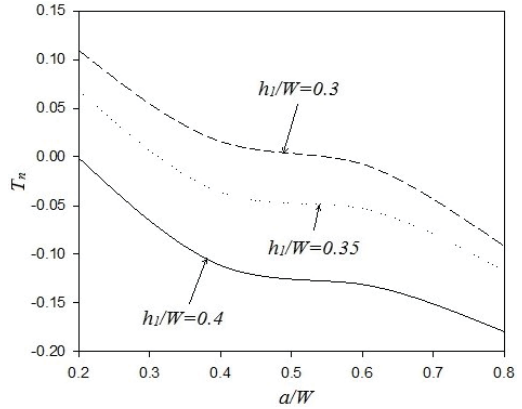

Fig. 15 Normalized T-stress for the model $w = 5, h = 2.5, P = 0.6, V_{f_0} = 0.1$

IV. Conclusion

Results indicate that generally crack propagation inhabitation is easily controllable in composites with variable spaced fibers, and comparison of the energy release rate in composites having the property $1/P = 0$ (equally spaced fibers) with those having P equal to other values, reveals that composites with variable fiber spacing are behaving quite better than equally spaced ones in every aspect.

T-stress is known as a critical factor as a crack parameter in analysis, which determines the crack kinking angle and also plastic zone size around crack tip. As a conclusion, investigation of T-stress would show accuracy of the results gained for the crack. It is quite clear from the results that the same explanations as energy release rate are not valid for T-stress outcomes of analysis, and functionally spaced fibers seem to have less accurate results than equally spaced ones, since in general, its magnitude is larger than T-stress value for FRC with variable fiber spacing.

References

[1] R. F. Gibson, *Principles of Composite Material Mechanics*. McGraw-Hill, Singapore, 1994.
[2] J. Hutchinson, "Singular behaviour at the end of a tensile crack in a hardening material," *Journal of the Mechanics and Physics of Solids*, vol. 16, no. 1, pp. 13 – 31, 1968.
[3] J. R. Rice, "A path independent integral and the approximate analysis of strain concentration by notches and cracks," *Journal of Applied Mechanics*, vol. 35, no. 2, pp. 379–386, 1968.
[4] J. Knowles and E. Sternberg, "On a class of conservation laws in linearized and finite elastostatics," *Archive for Rational Mechanics and Analysis*, vol. 44, no. 3, pp. 187–211, 1972.
[5] T. Hellen and W. Blackburn, "The calculation of stress intensity factors for combined tensile and shear loading," *International Journal of Fracture*, vol. 11, no. 4, pp. 605–617, 1975.
[6] B. Budiansky and J. R. Rice, "Conservation laws and energy-release rates," *Journal of Applied Mechanics*, vol. 40, no. 1, pp. 201–203, 1973.
[7] W.-H. Chen and K. Ting, "Finite element analysis of mixed-mode thermoelastic fracture problems," *Nuclear Engineering and Design*, vol. 90, no. 1, pp. 55 – 65, 1985.
[8] W. Chen and K. T. Chen, "On the study of mixed- mode thermal fracture using modified jk -integrals," *International Journal of Fracture*, vol. 17, p. R99R103, 1981.
[9] J. Chang and D. Wu, "Computation of mixed-mode stress intensity factors for curved cracks in anisotropic elastic solids," *Engineering Fracture Mechanics*, vol. 74, no. 8, pp. 1360 – 1372, 2007.
[10] S. Chu and C. Hong, "Application of the jk integral to mixed mode crack problems for anisotropic composite laminates," *Engineering Fracture Mechanics*, vol. 35, no. 6, pp. 1093 – 1103, 1990.
[11] E. Pan and B. Amadei, "Fracture mechanics analysis of cracked 2-d anisotropic media with a new formulation of the boundary element method," *International Journal of Fracture*, vol. 77, no. 2, pp. 161–174, 1996.
[12] P. Sollero and M. Aliabadi, "Fracture mechanics analysis of anisotropic plates by the boundary element method," *International Journal of Fracture*, vol. 64, no. 4, pp. 269–284, 1993.
[13] R. Khandelwal and J. C. Kishen, "Complex variable method of computing jk for bi-material interface cracks," *Engineering Fracture Mechanics*, vol. 73, no. 11, pp. 1568 – 1580, 2006.
[14] R. Khandelwal and J. M. C. Kishen, "Computation of thermal stress intensity factors for bimaterial interface cracks using domain integral method," *Journal of Applied Mechanics*, vol. 76, no. 4, pp. 041 010–041 010, 2009.
[15] ANSYS, *ANSYS Basic Analysis Procedures Guide, Release 5.4, Canonsburg, PA, USA*. Ansys Inc., USA, 1997.
[16] J. Eischen, "An improved method for computing the {J2} integral," *Engineering Fracture Mechanics*, vol. 26, no. 5, pp. 691 – 700, 1987.
[17] S. Dag, E. E. Arman, and B. Yildirim, "Computation of thermal fracture parameters for orthotropic functionally graded materials using jk-integral," *International Journal of Solids and Structures*, vol. 47, no. 2526, pp. 3480 – 3488, 2010.
[18] J.-H. Kim and G. H. Paulino, "Mixed-mode j-integral formulation and implementation using graded elements for fracture analysis of nonhomogeneous orthotropic materials," *Mechanics of Materials*, vol. 35, no. 12, pp. 107 – 128, 2003.
[19] S. Dag, "Mixed-mode fracture analysis of functionally graded materials under thermal stresses: A new approach using j k -integral," *Journal of Thermal Stresses*, vol. 30, no. 3, pp. 269–296, 2007.

[20] S. Dag, B. Yildirim, O. Arslan, and E. E. Arman, "Hygrothermal fracture analysis of orthotropic materials using j k -integral," *Journal of Thermal Stresses*, vol. 35, no. 7, pp. 596–613, 2012.
[21] J.-H. Kim and G. H. Paulino, "Finite element evaluation of mixed mode stress intensity factors in functionally graded materials," *International Journal for Numerical Methods in Engineering*, vol. 53, no. 8, pp. 1903–1935, 2002.